JPE 7-4-10

A Modularized Charge Equalization Converter for a Hybrid Electric Vehicle Lithium-Ion Battery Stack

Hong-Sun Park*, Chong-Eun Kim*, Chol-Ho Kim*, Gun-Woo Moon† and Joong-Hui Lee**

†*Department of Electrical Engineering and Computer Science, KAIST, Korea
**SK Institute of Technology, Korea

ABSTRACT

This paper proposes a modularized charge equalization converter for hybrid electric vehicle (HEV) lithium-ion battery cells, in which the intra-module and the inter-module equalizer are implemented. Considering the high voltage HEV battery pack, over approximately 300V, the proposed equalization circuit modularizes the entire $M*N$ cells; in other words, M modules in the string and N cells in each module. With this modularization, low voltage stress on all the electronic devices, below roughly 64V, can be obtained. In the intra-module equalization, a current-fed DC/DC converter with cell selection switches is employed. By conducting these selection switches, concentrated charging of the specific under charged cells can be performed. On the other hand, the inter-module equalizer makes use of a voltage-fed DC/DC converter for bi-directional equalization. In the proposed circuit, these two converters can share the MOSFET switch so that low cost and small size can be achieved. In addition, the absence of any additional reset circuitry in the inter-module equalizer allows for further size reduction, concurrently conducting the multiple cell selection switches allows for shorter equalization time, and employing the optimal power rating design rule allows for high power density to be obtained. Experimental results of an implemented prototype show that the proposed equalization scheme has the promised cell balancing performance for the 7Ah HEV lithium-ion battery string while maintaining low voltage stress, low cost, small size, and short equalization time.

Keywords: Hybrid electric vehicle (HEV), modularized charge equalization, lithium-ion battery

1. Introduction

The hybrid electric vehicle (HEV) has become one of the most promising cars in the automobile industry due to its energy saving ability and low emission of harmful pollutants [1]-[5]. An HEV can recover energy from the wheels, which had been wasted in the past, and reuse it to propel the vehicle at low speeds or provide extra power required during high acceleration. Additionally, a battery powered HEV does not emit air pollutants.

Most HEVs on the streets these days use nickel-metal hybrid (Ni-MH) batteries. Recent developments in the lithium-ion battery, which have been verified by test results, show that the lithium-ion battery has higher power and energy density, a lower self-discharge rate, and higher

Manuscript received Sept. 05, 2007; revised Sept. 05, 2007
† Corresponding Author: gwmoon@ee.kaist.ac.kr
Tel: +82-42-869-3475, Fax: +82-42-869-8520,
* Dept. of Electrical Engineering and Computer Science, KAIST
** SK Institute of Technology

single cell voltage than the Ni-MH battery. Therefore, it has great potential to take the place of the Ni-MH battery in the near future [4], [5]. However, to realize this possibility, reliability and safety need to be ensured; that is, the lithium-ion battery voltage and current limits should be maintained within allowable ranges to prevent permanent deterioration of performance and, in the worst case, explosion or fire in the vehicle.

Currently, continual charge and discharge of series connected battery cells can cause charge imbalance. The problem is that when cells are left in use without any control such as cell equalization, this unwanted circumstance can occur frequently. For example, in regenerative braking mode highly charged cells cannot capture an optimal amount of renewable energy. And in battery powered driving mode deeply discharged cells cannot provide sufficient stored energy. Therefore, charge equalization for the series connected battery cells is essential to prevent these undesirable situations, accomplish the maximum utilization of the battery, and prolong its lifetime [4]-[17]. Protection circuitry is, of course, important in battery management, but it is beyond the scope of this paper.

To achieve charge equalization for the battery string, plenty of algorithmic schemes and circuitry topologies have been developed [5]-[16] and are well summarized [6]. Among them, a resistive current shunt, which is connected across each cell and controlled by a micro-processor, has been presented. Simple implementation, low production cost, and stable operations are great advantages, but energy dissipation is a major drawback of this circuit [7].

To improve the energy consumption, non-dissipative charge equalization methods have been applied, in which charge-type, discharge-type, and charge- and discharge-type equalization are involved [8]-[16]. In charge-type equalization, under charged cells can receive energy from the overall battery stack automatically [8] or selectively [9]. This scheme is suitable for the case where a few of batteries are frequently under charged. On the other hand, in discharge-type equalization, extra energy from over charged cells is regenerated into the whole battery string [10] or removed to adjacent cells [11]. This is beneficial in the case where only a few cells are over charged. In charge- and discharge-type equalization, bi-directional equalization, in other words, energy from over charged cells flows into other under charged cells through current-fed DC/DC converters[12]-[14] or voltage-fed DC/DC converters [15], [16]. This method is more profitable for applications in which some batteries are under charged while others are over charged.

All of these non-dissipative cell balancing schemes show good equalization performance by employing high efficiency DC/DC converters. However, designing a cell balancing circuit using the above schemes for a HEV battery stack, with over approximately eighty cells and higher than 320V, will cause severe problems. For example, high voltage stress of electronic devices and high circulating energy may be experienced [10], [12]. In addition, establishing multiple windings within a single common core is a hard task [8], [9], [16]. Even if this were not so, cell balancing performance would degrade due to lots of energy conversions since over charged cells and under charged cells are sometimes far away from each other [11], [13]-[15].

To overcome these problems, a modularized charge equalization converter is proposed in this paper. In the proposed circuit, the intra-module and the inter-module equalizer are constructed for low voltage stress of all the electronic devices. Both the intra-module and the inter-module equalizer commonly use the MOSFET switch so that small size and low cost can be obtained. Besides, to achieve further size reduction, a current-fed DC/DC converter with cell selection switches is employed for intra-module cell balance, and a voltage-fed DC/DC converter with no additional reset circuitry is employed for inter-module equalization. The optimal power rating selection guide is also applied to achieve high power density, and the multiple cell selection switches can be turned on at the same time to obtain efficient charge equalization in a short time.

This paper is organized as follows. The modularized charge equalization converter for a HEV lithium-ion battery string is proposed in Section 2, where the intra-module and the inter-module equalization schemes are carefully described. Then, an optimal power rating design rule is considered for intra-module cell balance in Section 3. Experimental results of a prototype of the modularized equalization scheme employing the optimal

power rating design rule are shown in Section 4. Finally, concluding remarks are summarized in Section 5.

2. Proposed Charge Equalization Converter

Fig. 1 shows the proposed modularized charge equalization converter for a HEV battery pack, in which the inter-module and the intra-module equalizer are employed. For easy explanation, the proposed equalization scheme will be applied to a string of 4 cells. As shown in Fig. 1, the battery string is modularized into two modules and each module consists of two cells. In the intra-module equalizer, each cell has a flyback DC/DC converter with a cell selection switch at the primary side, and the two flyback converters within a module are coupled in parallel while commonly utilizing one MOSFET switch. On the other hand, the inter-module equalizer employs a voltage-fed DC/DC converter, where bi-directional equalizing current can be observed. One should note that there is no additional reset circuitry for the magnetizing current in this equalizer. This is because the equalizer can be reset by the under charged cells for which the corresponding cell selection switches are turned on.

The desirable features of the proposed charge equalization converter are as follows. First of all, by modularizing the battery stack, voltage stress on all the electronic components is reduced; the larger the number of modules and the smaller the number of cells in the module, the lower the voltage stress. Second, the intra-module and the inter-module equalizer share the MOSFET switch which reduces both the cost and size of the circuit. In addition, the intra-module equalizer employs the cell selection switch in place of the MOSFET switch and drive circuit, and the inter-module equalizer has no additional reset circuit. As a result, the implemented size of the proposed circuit can be further reduced. Third, a high power density equalizer can be constructed by using the optimal power rating design rule which is proposed in [17]. Lastly, an efficient equalization strategy and short balancing time can be accomplished owing to the cell selection switches. In other words, the intra-module equalizer can charge several under charged cells at the same time by conducting the corresponding cell selection switches.

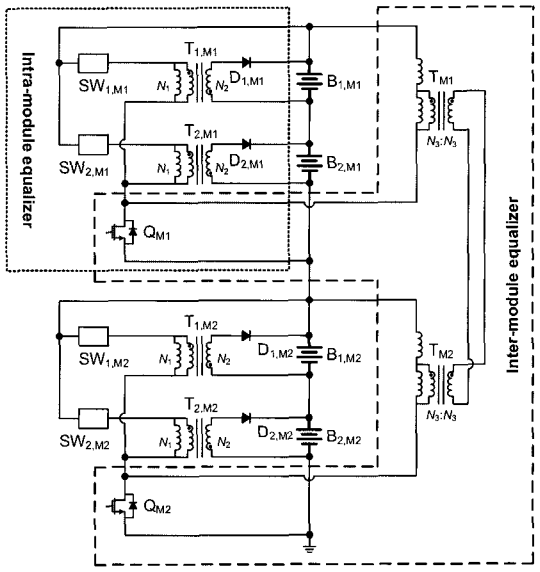

Fig. 1 Proposed modularized charge equalization converter

The operational principles of the modularized cell balancing circuit are composed of the superposition of the intra-module and inter-module equalizer. The operational modes of the proposed equalization circuit can be separated into four parts. Before describing mode 1, it is assumed that the upper module, M_1, is more under charged than the lower module, M_2, and the first cell in M_1 is the most under charged in the string. The cell selection switch, $SW_{1,M1}$, is turned on before the MOSFET switches, Q_{M1} and Q_{M2}, are turned on.

• **Mode 1(t_0-t_1):** When Q_{M1} and Q_{M2} are turned on at the same time, mode 1 starts. As shown in Fig. 2 and Fig. 3, the equalizing current transfers from M_2 to M_1 in the voltage-fed converter. The magnetizing current builds up at the magnetizing inductor of the first flyback DC/DC converter. The primary currents of the inter-module equalizers, $I_{kg,M1}$ and $I_{kg,M2}$, and the primary current of the intra-module equalizer, $I_{kg1,M1}$, can be given by:

$$I_{kg,M1}(t) = -\left(\frac{V_{M2} - V_{M1}}{L_{kg,M2} + L_{kg,M1}}\right)t \tag{1}$$

$$I_{kg,M2}(t) = \left(\frac{V_{M2} - V_{M1}}{L_{kg,M2} + L_{kg,M1}}\right)t + \frac{L_{kg,M2}V_{M1} + L_{kg,M1}V_{M1}}{L_{kg,M2} + L_{kg,M1}} \cdot \left(\frac{1}{L_{m,M2}} + \frac{1}{L_{m,M1}}\right)t \tag{2}$$

$$I_{kg1,M1}(t) = \left(\frac{V_{M1}}{L_{m1,M1}}\right)t \tag{3}$$

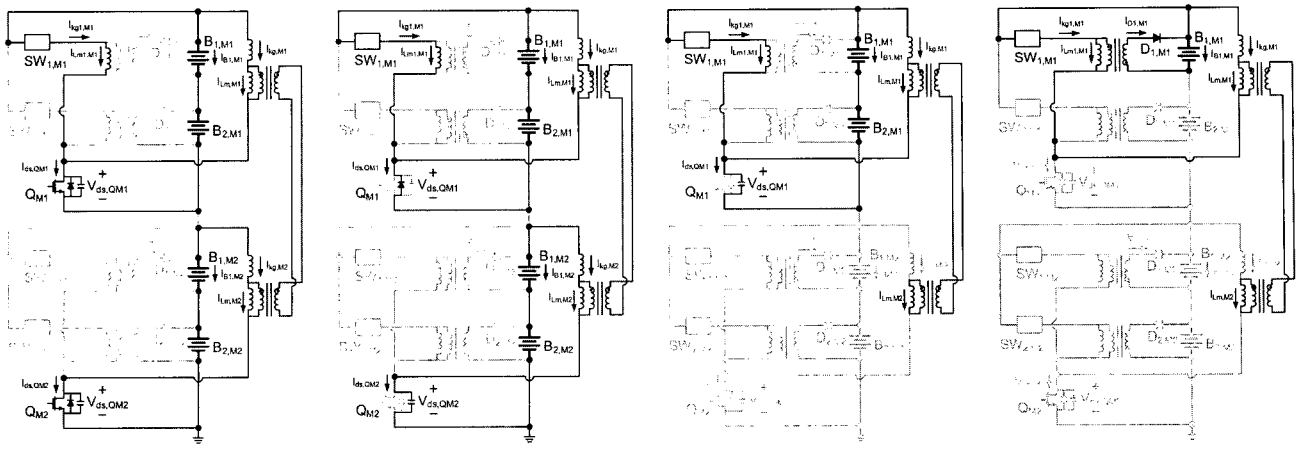

(a) (b) (c) (d)

Fig. 2 Operational modes of the proposed equalization converter. (a) Mode 1. (b) Mode 2. (c) Mode 3. (d) Mode 4.

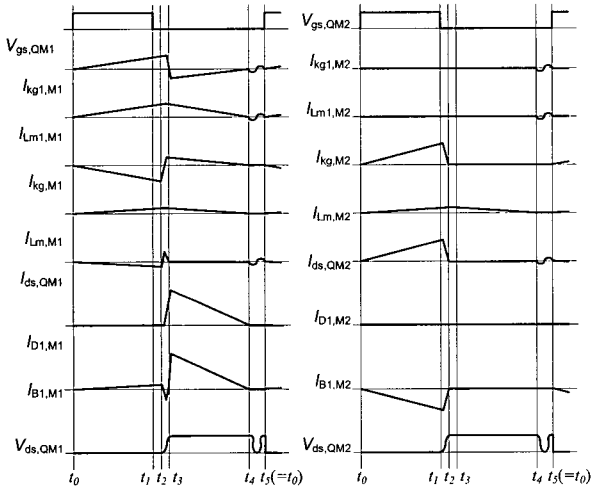

Fig. 3 Key waveforms of the proposed equalization converter

where two leakage inductors, $L_{kg,M1}$ and $L_{kg,M2}$, represent all the parasitic components within the transformers, T_{M1} and T_{M2}, respectively. The values of $L_{kg,M1}$ and $L_{kg,M2}$ are much smaller than those of the magnetizing inductors, $L_{m,M1}$ and $L_{m,M2}$, and V_{M1}. And V_{M2} are the voltages of M_1 and M_2.

• **Mode 2**(t_1-t_2): When Q_{M1} and Q_{M2} are synchronously turned off, mode 2 starts. In this mode, the output capacitor of Q_{M2} is fully charged. The voltage of the output capacitor, $V_{Coss,QM2}(t)$, can be approximately obtained by:

$$
\begin{aligned}
V_{Coss,QM2}(t) &= (V_{M2}-V_{M1})(1-\cos[\omega_1(t-t_2)]) \\
&+\left(\frac{V_{M2}-V_{M1}}{L_{kg,M1}+L_{kg,M2}}t_2\right)\sqrt{\frac{L_{kg,M1}+L_{kg,M2}}{0.5C_{oss,QM2}}}\sin[\omega_1(t-t_2)] \\
&+\frac{L_{kg,M2}V_{M1}+L_{kg,M1}V_{M1}}{L_{kg,M2}+L_{kg,M1}}\cdot\left(\frac{1}{L_{m,M2}}\right)\cdot t_2\cdot\sqrt{\frac{L_{m,M2}}{C_{oss,QM2}}}\sin[\omega_2(t-t_2)] \\
&+\frac{L_{kg,M2}V_{M1}+L_{kg,M1}V_{M1}}{L_{kg,M2}+L_{kg,M1}}\cdot\left(\frac{1}{L_{m,M1}}\right)\cdot t_2\cdot\sqrt{\frac{L_{m,M1}}{C_{oss,QM2}}}\sin[\omega_3(t-t_2)], \qquad t_2\le t\le t_3
\end{aligned}
\tag{4}
$$

where $C_{oss,QM1}=C_{oss,QM2}$, $\omega_1=1/\sqrt{0.5(L_{kg,M1}+L_{kg,M2})\cdot C_{oss,QM2}}$, $\omega_2=1/\sqrt{L_{m,M2}C_{oss,QM2}}$, and $\omega_3=1/\sqrt{L_{m,M1}C_{oss,QM2}}$.

• **Mode 3**(t_2-t_3): Mode 3 begins when the output capacitor of Q_{M1} is ready to be charged. The output capacitor of Q_{M1} is charged following the equalization below:

$$
\begin{aligned}
V_{Coss,QM2}(t) &= -(V_{M2}-V_{M1})(1-\cos[\omega_1(t-t_2)]) \\
&-\left(\frac{V_{M2}-V_{M1}}{L_{kg,M1}+L_{kg,M2}}t_2\right)\sqrt{\frac{L_{kg,M1}+L_{kg,M2}}{0.5C_{oss,QM1}}}\sin[\omega_1(t-t_2)] \\
&+\left(\frac{V_{M1}}{L_{m1,M1}}t_2\right)\sqrt{\frac{L_{m1,M1}}{C_{oss,QM1}}}\sin[\omega_4(t-t_2)], \qquad t_2\le t\le t_3
\end{aligned}
\tag{5}
$$

where $\omega_4=1/\sqrt{L_{m1,M1}C_{oss,QM1}}$. As shown in Fig. 2 and Fig. 3, Q_{M1} is completely turned off later than Q_{M2}. This is because only the leakage inductor of the first flyback DC/DC converter contributes to the turn-off process of Q_{M1}. On the other hand, in the case of Q_{M2}, there exists much energy which mainly comes from the two leakage

inductors and the two magnetizing inductors of the inter-module transformers.

• **Mode 4**(t_3-t_4): When the rectifier diode, $D_{1,M1}$, is turned on, mode 4 starts. In this mode, the magnetizing current, $I_{Lm1,M1}$, flows into the first cell which has previously been assumed to be the most under charged. This is the intra-module equalization process. In addition, there are additional equalizing currents, which are the magnetizing currents from the inter-module equalizer. In other words, the magnetizing currents are reset through the first cell voltage.

3. Design Considerations

In this section, to obtain high power density of the proposed circuit, the optimal power rating design rule will be applied. As described in [17], the optimal power rating selection guide can provide the minimal size of the cell balancing circuit while achieving equalization within the cell balancing time. In this paper, this power rating design rule will be applied only to the intra-module equalizer, not the inter-module equalizer since the inter-module equalization can be achieved automatically by using the voltage-fed DC/DC converter. Before applying the optimal power rating selection guide, it is noted that the proposed cell balancing circuit will be designed for 40 cells which are modularized into 5 modules. In addition, we assume that although nearly all the cells in the string are similar to each other, only a few cells are occasionally under charged.

Fig. 4 shows the battery model used for designing the optimal power rating of the proposed equalization circuit. The open circuit voltage of the commercial 7Ah lithium-ion battery is described according to the state of the charge (SOC). The dot symbol shows the experimental results from 10% to 90% in the SOC and the solid line is the linear approximation of the experimental observations in a least square sense. Among them, the recommended operation regions, approximately from SOC=30% to SOC=70%, are mainly considered. The following notations are very useful in this paper:

$Q_n(t)$: charge quantity of the nth cell at time t

$V_n(t)$: voltage of the nth cell at time t

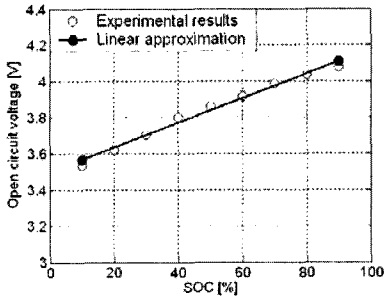

Fig. 4 The commercial 7Ah lithium-ion battery model

I_n: constant input current of the nth cell

I_{in}, I_{out}: constant input, output current of the intra-module equalizer

$P_{in}(t)$, $P_{out}(t)$: input power, output power of the intra-module equalizer at time t

$P_{in,avg}$, $P_{out,avg}$: average input power, average output power of the intra-module equalizer

η: overall efficiency of the intra-module equalizer.

To obtain the optimal power rating of the intra-module equalizer while achieving cell balance within an equalization time, the following simultaneous equations should be satisfied:

$$Q_1(t) = \frac{1}{7}\sum_{n=2}^{n=8} Q_n(t) \tag{6}$$

$$P_{out,avg} = \eta P_{in,avg}, \tag{7}$$

where only the first cell within a module is under charged. It is noted that by (6) and (7), the charge quantity left in the first cell at equalization time t is equal to the average charge quantity of the other cells, and the overall efficiency of the intra-module cell balancing circuit is η. In addition, the charge quantity left in the first cell at time t and the average output power of the intra-module equalizer can be given by:

$$Q_1(t) = Q_1(0) + I_1 \cdot t = Q_1(0) + (I_{out} - I_{in}) \cdot t \tag{8}$$

$$\begin{aligned} P_{out,avg} &= \frac{1}{t}\int_0^t P_{out}(\tau)d\tau = \frac{1}{t}\int_0^t V_1(\tau) I_{out} d\tau \\ &= \frac{1}{t}\int_0^t \left(V_1(0) + \frac{(I_{out} - I_{in})\cdot\tau}{C}\right) I_{out} d\tau \\ &= \left(V_1(0) + \frac{1}{2C}(I_{out} - I_{in})\cdot t\right)\cdot I_{out}, \end{aligned} \tag{9}$$

where C is the capacitance of the 7Ah lithium-ion battery used in this paper. In addition, the average power is taken into account since the cell voltages can change during the equalization process, even if only a little bit.

Fig. 5 shows the simulation results of the optimal power rating, where the equalization time is plotted into the intra-module equalizer according to the input current, and the net regenerated current which flows into the first cell. In this simulation, the various efficiencies of the intra-module equalization circuit are considered as simulation parameters. In addition, the initial SOC difference between the under charged cell and the other cells is assumed to be between 10% and 20%.

The simulation results show that the larger input current into the intra-module equalizer takes a shorter equalization time and provides the higher equalizing current. In addition, the larger the SOC difference, the longer the equalization time, and the higher the efficiency of the balancing circuit, the shorter the equalization time. For example, when applying the balancing circuit of η=80%, an equalization time of about 2 hours is required to achieve charge equalization provided that the input current of 0.12A flows into the intra-module equalizer for the SOC difference of 20% as shown in Fig. 5(c). In this case, the net equalizing current into the first cell is approximately 600mA.

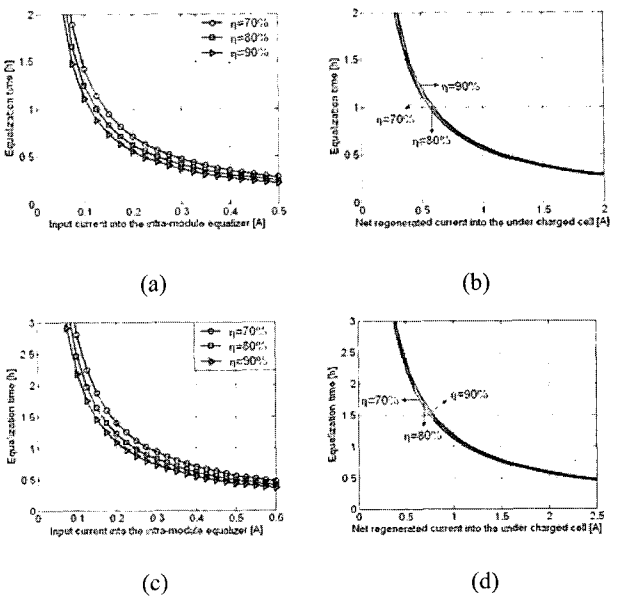

Fig. 5 Simulation results of the optimal power rating design. (a) Equalization time vs. input current for SOC difference of 10%. (b) Equalization time vs. regenerated current for SOC difference of 10%. (c) Equalization time vs. input current for SOC difference of 20%. (d) Equalization time vs. regenerated current for SOC difference of 20%.

4. Experimental Results

To verify the operational principles of the proposed cell balancing circuit and the usefulness of the optimal power rating design rule, a prototype is implemented. Its photograph is shown in Fig. 6. The intra-module equalizer is employed within a module of 8 cells for charge balance, and the inter-module equalizer among 5 modules for module balance. The intra-module equalizer is designed using the optimal power rating selection guide. In this prototype, commercial 7Ah lithium-ion batteries of 40 cells are used for the HEV battery system. The parameters used for constructing the prototype are summarized in Table I.

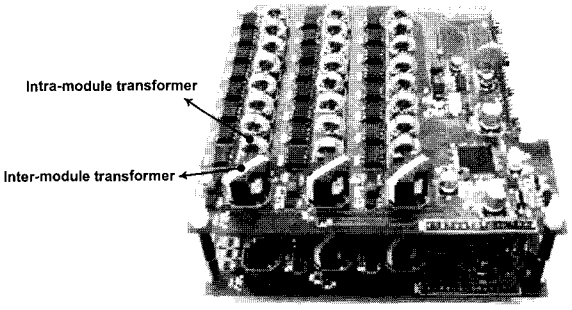

Fig. 6 Photograph of the implemented prototype

Fig. 7 shows the experimental key waveforms of the implemented prototype, where only two modules are driven to carefully verify the operational principles of the intra-module and inter-module equalizer. The battery environment for this experiment is as follows. The voltage of the first module is 29.6V with SOC=28.9% and the second module is 30.9V with SOC=49.4%. Moreover, the first cell in the first module is the most under charged so that the cell selection switch, $SW_{1,M1}$, is turned on in advance. As shown in Fig. 7(a), the magnetizing current of the intra-module equalizer flows into the first cell through the rectifier diode, $D_{1,M1}$, during the turn-off period of a MOSFET switch. In addition, the magnetizing current of

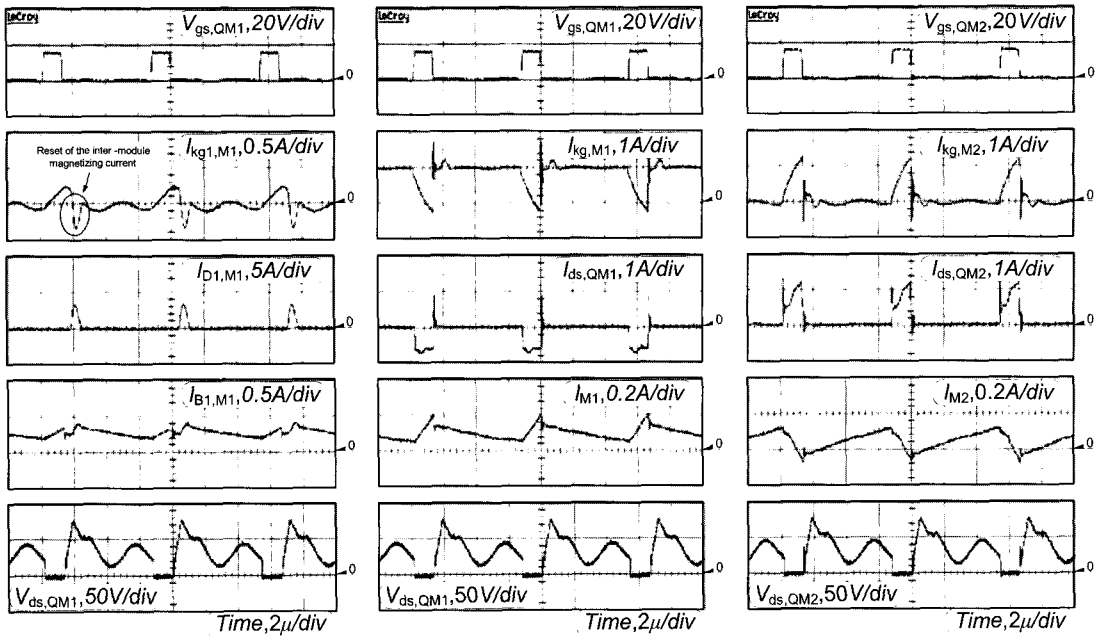

Fig. 7 Experimental key waveforms of the prototype for the first two modules

the inter-module equalizer is reset through the voltage of the first cell. The inter-module charge equalization can be also observed as shown in Fig. 7(b). The equalizing current flows from the second module into the first during the turn-on period of the MOSFET switches. The maximum voltage stress of the proposed equalization circuit resides at the MOSFET switches and its value does not exceed 80V including the voltage spikes. From these results, one can see that the proposed balancing circuit has advantageous features such as low voltage stress due to modularization and efficient equalization during the entire equalization time.

To show the cell balancing performance of the modularized charge equalization circuit, the equalization test is conducted for the commercial 7Ah lithium-ion battery cells. In this test, 40 cells are divided into 5 modules where each module consists of 8 cells. The SOC of the two most under charged cells is 24.8% for one and 33.5% for the other. In this equalization test, an intelligent battery management system (BMS) is employed and its control strategy is as follows. First, the BMS detects the most under charged cell, and then charges it until its SOC increase to the average SOC of the other cells. Second,

Table 1 Parameters used for the implemented prototype

Parameters			Value
Intra-module equalizer	Selection switch, $SW_{1,M1}$- $SW_{8,M5}$		PS710EL-A
	Diode, $D_{1,M1}$- $D_{8,M5}$		STPS2L30A
	MOSFET, Q_{M1}-Q_{M5}		IRF7495
	Floating Gate Driver		HCPL-3140
	Transformer, $T_{1,M1}$- $T_{8,M5}$	Core	CM102173
		N_1:N_2	39:5
		L_m, L_{kg}	127μH, 2.8μH
Inter-module equalizer	Transformer, T_{M1}- T_{M5}	Core	RN41812
		N_3:N_3	14:14
		L_m, L_{kg}	500μH, 200nH
Lithium-ion battery string	Capacity		7Ah
	SOC of B_{39} at t=0		24.8%
	SOC of B_{10} at t=0		33.5%
	SOC of the other cells at t=0	Max.	46.7%
		Min.	24.8%
		Mean	40.0%

after finishing the first step, the BMS will charge the next most under charged cell in the same way. Lastly, these two steps are repeated until all the voltages in the string are within 50mV.

Fig. 8 shows the equalization performance of the proposed modularized balancing circuit; the first 2 hours of the equalization time is used for charging the 39th cell, the next 47 minutes for the 10th cell, and then the last 18 minutes for the next most under charged cell. As shown in Fig. 8, the initial SOC difference of 21.9% decreases to 5.4% at the end of equalization. It is remarkable that in the case of the 39th cell, the average equalizing current is measured to be 600mA. This value is very similar to the simulation result shown in Fig. 5(d). From this result, the proposed charge equalization circuit, implemented by using the optimal power rating design rule, shows outstanding charge balancing performance within a high power density.

5. Conclusions

When designing a cell balancing circuit for a high voltage HEV lithium-ion battery system, voltage stress of electronic components, circuit size, production cost, and implementation problems are the major design parameters. To satisfy these requirements, a modularized charge equalization converter was proposed in this paper. In the proposed circuit, low voltage stress of all the electronic devices was achieved by modularizing the entire cells. Moreover, small size and low production cost can be obtained due to common use of the MOSFET switches by the intra-module and the inter-module equalizer, the use of cell selection switches at the intra-module equalizer, and the absence of an additional reset circuit at the inter-module equalizer. In addition, by employing the optimal power rating design rule, the proposed balancing circuit can be constructed in high power density. Finally, all the magnetic components can be easily implemented, and a simple equalization strategy intended for only the intra-module equalization can be employed. From these good points, the modularized charge equalization converter proposed in this paper can be widely applied to the high voltage series connected battery stack such as HEV and EV.

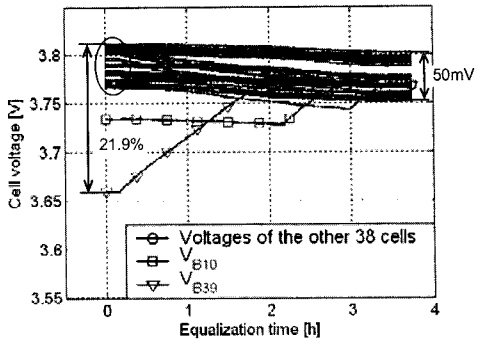

Fig. 8 Equalization performance of the proposed cell balancing circuit

Acknowledgment

This work was supported through research funding by SK Corporation, Republic of Korea.

References

[1] A. Emadi, S. Williamson, and A. Khaligh, "Power electronics intensive solutions for advanced electric, hybrid electric, and fuel cell vehicular power systems," *IEEE Trans. Power Electron.*, vol. 21. pp. 567-577, May 2006.

[2] S. Williamson, A. Emadi, and K. Rajashekara, "Comprehensive efficiency modeling of electric traction motor drives for hybrid electric vehicle propulsion applications," *IEEE Trans. Veh. Tech.*, vol. 56. pp. 1561-1572, July 2007.

[3] J. M. Miller, "Hybrid electric vehicle propulsion system architecture of the e-CVT type," *IEEE Trans. Power Electron.*, vol. 21. pp. 756-767, May 2006.

[4] A. Affanni, A. Bellini, G. Franceschini, P. Guglielmi, and C. Tassoni, "Battery choice and management for new-generation electric vehicles," *IEEE Trans. Ind. Electron.*, vol. 52, pp. 1343-1349, Oct. 2005.

[5] B. T. Kuhn, G. E. Pitel, and P. T. Krein, "Electrical properties and equalization of lithium-ion cells in automotive applications," in *Proc. 2005 IEEE Vehicle Power and Propulsion Conf.*, Chicago, USA, Sep. 2005, pp. 55-59.

[6] N. H. Kutkut and D. M. Divan, "Dynamic equalization techniques for series battery stacks," in *Proc. 18th Annu. Int. Telecommunications Energy Conf.*, Boston, USA, Oct. 1996, pp. 514-521.

[7] B. Lindemark, "Individual cell voltage equalizers (ICE) for reliable battery performance," in *Proc. 13th Annu. Int. Telecommunications Energy Conf.*, Kyoto, Japan, Nov.

1991, pp. 196-201.

[8] N. H. Kutkut, H. L. N. Wiegman, D. M. Divan and D. W. Novotny, "Design considerations for charge equalization of an electric vehicle battery system," *IEEE Trans. Ind. Appl.*, vol. 35, pp. 28-35, Feb. 1999.

[9] M. Tang and T. Stuart, "Selective buck-boost equalizer for series battery packs," *IEEE Trans. Aerosp. Electron. Syst.*, vol. 36, pp. 201-211, Jan. 2000.

[10] D. C. Hopkins, C. R. Mosling, and S. T. Hung, "Dynamic equalization during charging of serial energy storage elements," *IEEE Trans. Ind. Appl.*, vol. 29, pp. 363-368, Mar.-Apr. 1993.

[11] N. H. Kutkut, H. Wiegman, and R. Marion, "Modular battery charge equalizers and method of control," U.S. Patent 6 150 795, Nov. 21, 2000.

[12] H. Schmidt and C. Siedle, "The charge equalizer-a new system to extend battery lifetime in photovoltaic system, U.P.S. and electric vehicle," in *Proc. 15th Annu. Int. Telecommunications Energy Conf.*, Paris, France, Sep. 1993, pp. 144-151.

[13] Y.-S. Lee and G.-T. Cheng, "Quasi-resonant zero-current-switching bidirectional converter for battery equalization applications," *IEEE Trans. Power Electron.*, vol. 21, pp. 1213-1224, Sep. 2006.

[14] N. H. Kutkut, "A modular non dissipative current diverter for EV battery charge equalization," in *Proc. 13th Annu. Appl. Power Electron. Conf. and Exp.*, Anaheim, USA, Feb. 1998, pp. 686-690.

[15] P. T. Krein, S. West, and C. Papenfuss, "Equalization requirements for series VRLA battery," in *Proc. 16th Annu. Battery Conf. on Applications and Advances*, Long Beach, USA, Jan. 2001, pp. 125-130.

[16] N. H. Kutkut, "Non-dissipative current diverter using a centralized multi-winding transformer," in *Proc. 28th Power Electron. Specialists Conf.*, St. Louis, USA, June1997, pp. 648-654.

[17] H. -S. Park, C. -E. Kim, G. -W. Moon, J. -H. Lee, and J. K. Oh, "Two-stage cell balancing scheme for hybrid electric vehicle Lithium-ion battery strings," in *Proc. 38th Power Electron. Specialists Conf.*, Orlando, USA, June 2007.

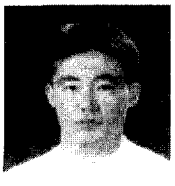

Hong-Sun Park was born in Korea, in 1974. He received the B.S. degree in Electronic Engineering from Sogang University, Seoul, Korea, in 2000 and the M.S. degree in Electrical Engineering from Korea Advanced Institute of Science and Technology (KAIST), Daejeon, in 2003. He is currently a Ph.D candidate in Electrical Engineering from KAIST. His research areas include design and control of HEV BMS, charge equalization converters, and low voltage high current DC/DC converters. Mr. Park is a student member of IEEE and a member of the Korea Institute of Power Electronics (KIPE).

Chong-Eun Kim received the B.S. degree in Electrical Engineering from Kyungpook National University, Daegu, Korea, in 2001. In 2003, he received the M.S. degree in Electrical Engineering from the Korea Advanced Institute of Science and Technology (KAIST), Daejeon, Korea, where he is currently working toward the Ph.D. degree. His main research interests are DC/DC converters, power-factor-correction (PFC) AC/DC converters, soft switching techniques, plasma display panels (PDP), and digital audio amplifiers.

Chol-Ho Kim was born in Iksan, Korea, in 1982. He received the B.S. degree from the School of Electrical Engineering and Computer Science at the Korea Advanced Institute of Science and Technology (KAIST), Daejeon, Korea, in 2005. He is currently taking towards his M.S. degree. His research areas of interest are design and control of HEV BMS, charge equalization converters, and low voltage high current DC/DC converters. Mr. Kim is a student member of IEEE and a member of the Korea Institute of Power Electronics (KIPE).

Gun-Woo Moon was born in Korea in 1966. He received the B.S. degree from Han-Yang University, Seoul, Korea, in 1990, and the M.S. and Ph.D. degrees in Electrical Engineering from the Korea Advanced Institute of Science and Technology (KAIST), Daejeon, Korea, in 1992 and 1996, respectively. He is currently an assistant professor in the department of Electrical Engineering and Computer Science at KAIST. His research interests include modeling, design and control of power converters, soft switching power converters, resonant inverters, distributed power systems, power factor corrections, electrical drive systems, driver circuits of PDP and flexible AC transmission systems (FACTS). Dr. Moon is an associate member of IEEE, a member of the Korea Institute of Power Electronics (KIPE), the Korea Institute of Electrical Engineering (KIEE), the Korea Institute of Telematics and Electronics (KITE), and the Korea Institute of Illumination Electronics and Industrial Equipment (KIIEIE).

Joong-Hui Lee was born in Seoul, Korea, in 1963. He received the B.S. degree and the M.S. degree in Electrical Engineering from Seoul National University, in 1987 and 1989, respectively, and the Ph.D degree in Electrical Engineering from Korea Advanced Institute of Science and Technology (KAIST), Daejeon, Korea, in 2003. He has worked for the SK Institute of Technology since 1989 and is currently a principal engineer at the HEVB System Development TF. His research areas include modeling and control of electric drive systems, charge equalizer and management systems for HEV batteries, and low power high efficiency DC/DC converters. Dr. Lee is a member of the Korea Institute of Power Electronics (KIPE).